Passive Cavity Surface–Emitting Lasers: Option of Temperature–Insensitive Lasing Wavelength for Uncooled Dense Wavelength Division Multiplexing Systems

V. A. Shchukin[a,b], N. N. Ledentsov[a,b], T. Slight[c], W. Meredith[c], N. Yu. Gordeev[b,d], A. M. Nadtochy[b,d], A. S. Payusov[b,d], M. V. Maximov[b,d], S. A. Blokhin[b], A. A. Blokhin[b], Yu. M. Zadiranov[b], N. A. Maleev[b], V. M. Ustinov[b], and K. D. Choquette[e]

[a] VI Systems GmbH, Hardenbergstr. 7, Berlin 10623, Germany
[b] A. F. Ioffe Physical Technical Institute, Politekhnicheskaya 26, St. Petersburg 194021, Russia
[c] Compound Semiconductor Technology, 4 Stanley Boulevard, Hamilton, G72 0BN, Scotland, UK
[d] St. Petersburg Academic University — Nanotechnology Research and Education Centre, Khlopina 8/3, St. Petersburg 194251, Russia
[e] University of Illinois at Urbana–Champaign, 208 N. Wright Street, Urbana IL 61801, USA

ABSTRACT

A concept of passive cavity surface–emitting laser is proposed aimed to control the temperature shift of the lasing wavelength. The device contains an all–semiconductor bottom distributed Bragg reflector (DBR), in which the active medium is placed, a dielectric resonant cavity and a dielectric top DBR, wherein at least one of the dielectric materials has a negative temperature coefficient of the refractive index, $dn/dT < 0$. This is shown to be the case for commonly used dielectric systems SiO_2/TiO_2 and SiO_2/Ta_2O_5. Two SiO_2/TiO_2 resonant structures having a cavity either of SiO_2 or TiO_2 were deposited on a substrate, their optical power reflectance spectra were measured at various temperatures, and refractive index temperature coefficients were extracted, $dn/dT = 0.0021$ K^{-1} for SiO_2 and $dn/dT = -0.0092$ K^{-1} for TiO_2. Using such dielectric materials allows designing passive cavity surface–emitting lasers having on purpose either positive, or zero, or negative temperature shift of the lasing wavelength $d\lambda/dT$. A design for temperature–insensitive lasing wavelength ($d\lambda/dT = 0$) is proposed. Employing devices with temperature–insensitive lasing wavelength in wavelength division multiplexing systems may allow significant reducing of the spectral separation between transmission channels and an increase in number of channels for a defined spectral interval enabling low cost energy efficient uncooled devices.

Keywords: passive cavity surface–emitting laser, refractive index thermal coefficient, dielectric cavity, dielectric distributed Bragg reflector, negative temperature shift of cavity resonance, temperature–insensitive lasing wavelength.

1. INTRODUCTION

The bandwidth density scaling occurs faster than the single channel data transmission rate. Consequently the number of channels per link increases. To counteract this trend two options are being pursued. One option is the development of faster optical devices and applying more complex modulation schemes and error correction protocols. This trend, beyond certain scaling limits, is restricted by the need of developing both faster optical devices and/or much more advanced and power hungry electronics. Such an approach is not economically feasible particularly if the optical channel speed exceeds the onboard speed of the related copper interfaces which is defined by the speed of the input–output interfaces of the related electronics.

Presently the number of channels in Ethernet links has increased from 1 to 10 parallel channels. The multimode fiber connectors become bulky and restrict the bandwidth density scaling. Another approach is applied in long reach links

Vertical-Cavity Surface-Emitting Lasers XX, edited by Kent D. Choquette, James K. Guenter, Proc. of SPIE Vol. 9766, 976609 · © 2016 SPIE
CCC code: 0277-786X/16/$18 · doi: 10.1117/12.2208915

using wavelength division multiplexing approach. In this case 4 or 10 channels in the 1300 nm wavelength range are multiplexed into a single mode fiber and at the other end of the transmission line demultiplexed to the related number of photodetectors. One should note that such approach is limited by a much higher cost and power consumption of such links. As more than 90% of the links in datacenters are shorter than 50 m, multimode fiber links dominate. The present trend is the transition from single duplex multimode fiber links in 10G Ethernet and Fibre Channel (4GFC, 8GFC, 16GFC, 32GFC) to 4 channel links (40G Ethernet at 10Gb/s per channel, 100G Ethernet as 25Gb/s, 128GFC at 28Gb/s). Further increase in the number of links is difficult. In 2008 it was proposed to apply two channels within the 840–860nm window over OM3 multimode fiber (MMF) to reach 40Gb/s per single duplex fiber [1]. It was also proposed to extend this approach up to 4 channels [2].

The idea [1,2] proposed in 2008 evoked recently a big interest of industry. Two channels transmission over a MMF was realized by CISCO [3]. Finisar reached 100Gb/s over single duplex fiber at 4 wavelength channels [4].

One should note however that the installed MM fiber has a maximum modal bandwidth only in the range 840–860 nm. Assuming the spectral width of uncooled VCSELs, the uncertainty in the angle of the emission due to multimode operation and the necessity of a certain wavelength spacing to exclude cross talk between the channels placing of more than two channels is difficult. Presently new broadwave MMF in the 850–950 nm range is under standardization to allow 4 channels at 30 nm spacing. The most of this is due to the temperature induced shift of the VCSEL. In a temperature range between –20^{o}C and 85^{o}C the shift is ~7 nm. Assuming a VCSEL wavelength uncertainty of 4 nm and 7 nm spacing to exclude cross talk between the channels one should allow at least 17 nm spacing. As the VCSEL is multimode, the angle uncertainty of the emission broadens the filter response and adds another 10 nm.

However, if VCSEL is made single mode and the temperature shift is eliminated, for the same 4 nm wavelength uncertainty and, assuming the spectral performance of the filters of 7 nm 10 channels can be placed within the 850–950 nm window. Consequently the bandwidth capacity per fiber can be more than doubled. Furthermore within a standard MMF having a maximum modal bandwidth at 840–860 nm, one can place 4 channels, for example, allowing long distance 100G transmission at 25 Gb/s. Virtually unlimited number of channels can be multiplexed using more advanced multiplexing systems.

Various concepts of semiconductor diode lasers were proposed in which the lasing wavelength was controlled by coincidence of two resonant features. Thus, the lasing wavelength of a tilted cavity laser [5] is controlled by the coincidence of the angular–dependent cavity resonance and angular–dependent reflectivity maximum within the reflectivity stopband of a multilayer interference reflector. A possibility to control of temperature dependence of the lasing wavelength including temperature–insensitive wavelength was theoretically predicted [6], and the approach modeled for an edge–emitting laser can be also extended to surface emitters. Another possibility is a filter–VCSEL [7], in which the lasing wavelength is controlled by the coincidence of two angular–dependent resonances of two coupled cavities. However, these approaches require much more calibration steps and more precise epitaxial growth than conventional VCSELs. Thus, a simple and straightforward approach to a surface emitting laser with temperature–independent lasing wavelength is highly needed.

2. PASSIVE CAVITY LASER TO CONTROL LASING WAVELENGTH TEMPERATURE SHIFT

In the present paper we explore a possibility to control temperature behavior of the lasing wavelength based on the concept of passive cavity laser. Shifting of the gain medium in surface–emitting lasers from the resonance cavity to a distributed Bragg reflector (DBR) enables new functionalities of surface–emitting devices [8,9]. First, once gain medium is placed in a bottom DBR, both the resonance cavity and the top DBR can be formed of dielectric material (the cavity is just a passive cavity), and the cavity can be etched through forming a photonic crystal device, in which modifications of the optical modes are much stronger than in conventional photonic crystal VCSELs [10] where only a part of the top DBR is etched. Second, the thermal shift of the lasing wavelength is now controlled by temperature dependence of the refractive indices of dielectric materials. And as, contrary to semiconductors with positive temperature coefficients of the refractive indices, dielectric materials are known with both positive and negative temperature coefficients. This fact creates a possibility to configure a passive dielectric cavity and a top dielectric DBR such that a negative change of the refractive indices of the dielectric part of the device compensates a positive change in the semiconductor part leading to temperature–insensitive lasing wavelength.

Such dielectric materials like Barium Borate glass E1583 (mixture of B_2O_3 and BaO) [11], Thallium Bromide–Thallium Iodide Mixture (KRS–5) [12], NPK–51 or Lithotec CaF_2 [13], etc. are known to have negative temperature coefficients

of the refractive indices, $dn/dT<0$. In the present paper we investigate other dielectric materials that are common for using in multilayer coatings for semiconductor lasers.

3. REFRACTIVE INDEX TEMPERATURE COEFFICIENTS OF SiO_2 AND TiO_2

To investigate refractive index temperature coefficients of two dielectric materials, namely SiO_2 and TiO_2, we extend the method of Ref. [14] to our system. The approach include fabrication of two resonant structures containing a resonant cavity of a first or of a second of two materials, sandwiched between two DBRs formed of the same materials, measuring the optical power reflectance spectra versus temperature, extracting the shift of the reflectivity dip upon temperature, modeling such shift assuming unknown values of dn/dT for each of the materials and extracting these values from fitting the modeled shift of the dips to the measured data.

One should note however, a significant difference from [14]. In Ref. [14] the GaAs/AlAs resonant structures contained 10λ–cavities formed of either GaAs or AlAs. However, as the accuracy of dielectric deposition is commonly lower than the accuracy of the semiconductor epitaxial growth, the deposition of such thick cavity is hardly possible. Indeed, an increased thickness of the cavities (not just λ/2) is needed to make two structures distinguishable in the temperature shifts of the optical resonance. However, as the relative refractive index step for dielectric structures ($|n_2–n_1|/(n_1+n_2)$ = 0.22) is larger than that for semiconductor structures ($|n_2–n_1|/(n_1+n_2)$ = 0.08) the dielectric structures become distinguishable at significantly thinner cavities. For our studies we use structures with 2λ–cavities.

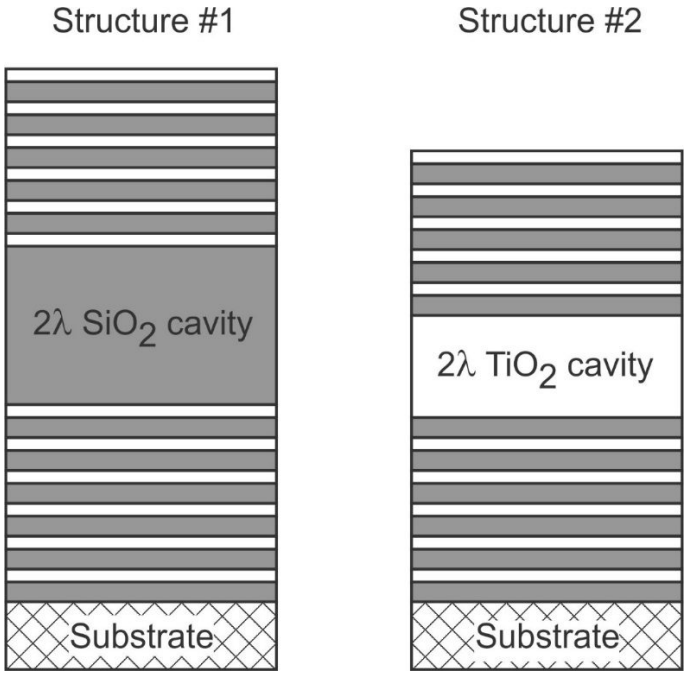

Fig.1. Two test resonance structures formed of 2λ–cavity placed between two distributed Bragg reflectors.

Figure 1 shows schematically two deposited resonance dielectric structures containing either 2λ SiO_2 or 2λ TiO_2 cavity placed between two DBRs composed of alternating λ/4 layers of low–index (SiO_2) and high–index (TiO_2) materials.

Figure 2(a) demonstrates cross–sectional scanning electron microscopy (SEM) image of the deposited resonant test structure #1. The SEM image confirms a good morphology of the multilayer dielectric structure. Figure 2(b) depicts the measured optical power reflectance (OR) spectrum having a reflectivity dip within the stopband (marked by a dashed ellipsis). This is the dip, the temperature shift of which was measured.

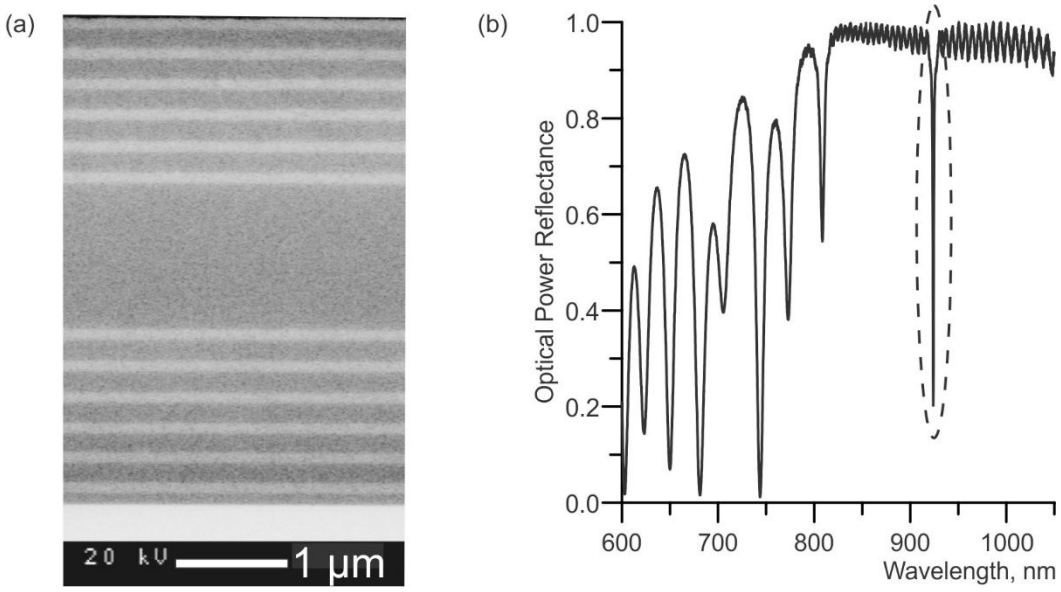

Fig.2. (a) Cross–sectional scanning electron microscopy image of the test resonance structure #1 of Fig. 1 containing SiO_2 cavity. (b) Optical power reflectance spectrum of the structure #1.

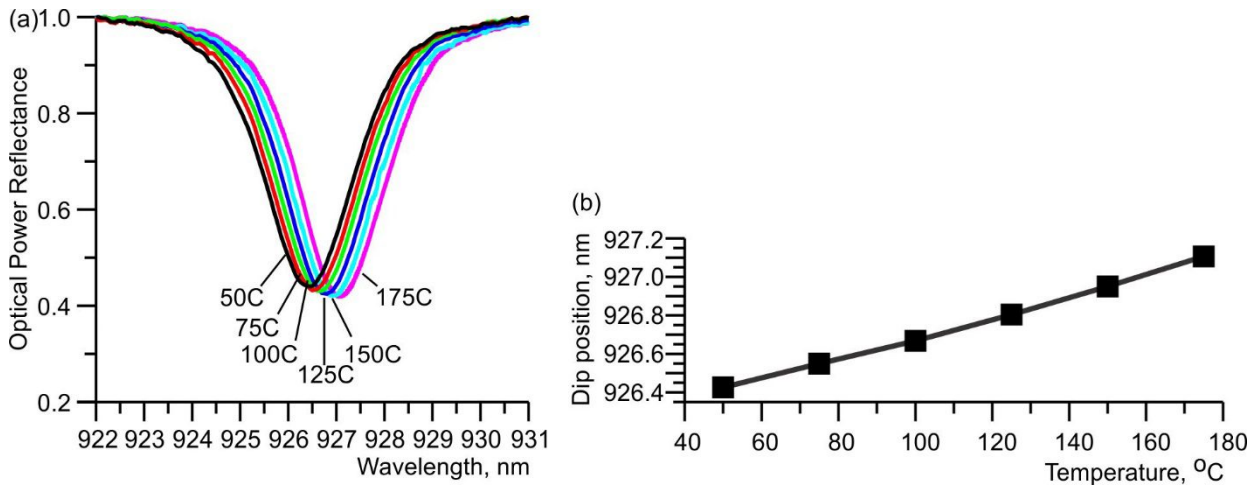

Fig.3. (a) Optical power reflectance spectra of Structure #1 of Fig. 1 containing SiO_2 cavity in the vicinity of the reflectivity dip at various temperatures. (b) Temperature shift of the dip position.

Figure 3(a) depicts the OR spectra of Structure #1 in the vicinity of the reflectivity dip at various temperatures, and Figure 3(b) shows the shift of the dip versus temperature. The shift is approximately linear. It is a small positive shift at a rate of 0.005 nm/K which is about 10 times smaller than the shift in typical semiconductor structures.

Figure 4 shows the measured OR spectrum of Structure #2 of Fig. 1. The dashed ellipsis marks the reflectivity dip the temperature shift of which was studied. Figure 5(a) depicts the OR spectra of Structure #2 in the vicinity of the reflectivity dip at various temperatures. The shift of the dip versus temperature reveals a certain non–linearity. Once this dependence is approximated by a linear function, this gives a significant negative shift of the dip at a rate –0.02 nm/K.

In order to extract the refractive index temperature coefficients from the OR measurements, the shift of the reflectivity dip was modeled, and all sources of the shift were taken into account including changes in the refractive indices of materials 1 and 2 as well as thermal expansion of materials 1 and 2,

$$\frac{d\lambda_1^{dip}}{dT} = \left(\frac{\partial\lambda_1^{dip}}{\partial n_1}\right)\frac{dn_1}{dT} + \left(\frac{\partial\lambda_1^{dip}}{\partial n_2}\right)\frac{dn_2}{dT} + \left(\frac{\partial\lambda_1^{dip}}{\partial d_1}\right)d_1\alpha_1 + \left(\frac{\partial\lambda_1^{dip}}{\partial d_2}\right)d_2\alpha_2 , \quad (1a)$$

$$\frac{d\lambda_2^{dip}}{dT} = \left(\frac{\partial\lambda_2^{dip}}{\partial n_1}\right)\frac{dn_1}{dT} + \left(\frac{\partial\lambda_2^{dip}}{\partial n_2}\right)\frac{dn_2}{dT} + \left(\frac{\partial\lambda_2^{dip}}{\partial d_1}\right)d_1\alpha_1 + \left(\frac{\partial\lambda_2^{dip}}{\partial d_2}\right)d_2\alpha_2 . \quad (1b)$$

Here the first and the second terms on the right hand side of Eqs.(1a) and (1b) stand for the contributions of the change in refractive index of material 1 and 2, respectively. The third and the fourth terms refer to the contributions to the dip shift of the thermal expansion of material 1 and 2, respectively, α_1 and α_2 being thermal expansion coefficients, d_1 and d_2 refer schematically to the plurality of the thicknesses of the layers of materials 1 and 2.

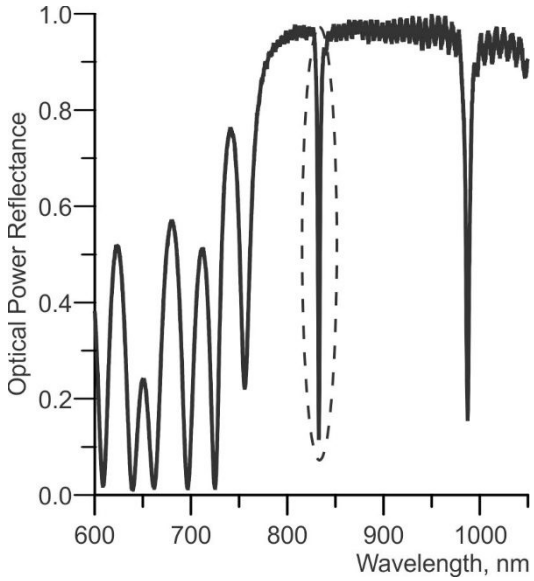

Fig.4 Optical power reflectance spectrum of the structure #2 of Fig. 1 containing TiO_2 cavity.

Refractive indices measured at room temperature at wavelengths close to 850 nm were 1.45 for SiO_2 and 2.25 for TiO_2, and for chromatic dispersion the values $dn/d\lambda = -1.6\text{x}10^{-5}$ nm^{-1} and $dn/d\lambda = -2.0\text{x}10^{-4}$ nm^{-1}were used for SiO_2 and TiO_2 respectfully [15]. The values reported for thermal expansion coefficient of SiO_2 range typically between $4.1\text{x}10^{-6}$ K^{-1} and $5.0\text{x}10^{-6}$ K^{-1} [16,17], we assumed $4.5\text{x}10^{-6}$ K^{-1}. The values for TiO_2 range between $8.4\text{x}10^{-6}$ K^{-1} and $11.8\text{x}10^{-6}$ K^{-1} [18], we assumed $9.2\text{x}10^{-6}$ K^{-1} following [19]. The modeling yields the following values for the refractive index temperature coefficients

For SiO_2 $\frac{dn}{dT} = 0.0021$ K^{-1}, and (2a)

for TiO_2 $\frac{dn}{dT} = -0.0092$ K^{-1}. (2b)

A large negative temperature coefficient of the refractive index of TiO_2 gives a possibility to apply these two materials for passive cavity surface emitting laser having a dielectric cavity and a dielectric top DBR and thus effectively control the temperature shift of the lasing wavelength.

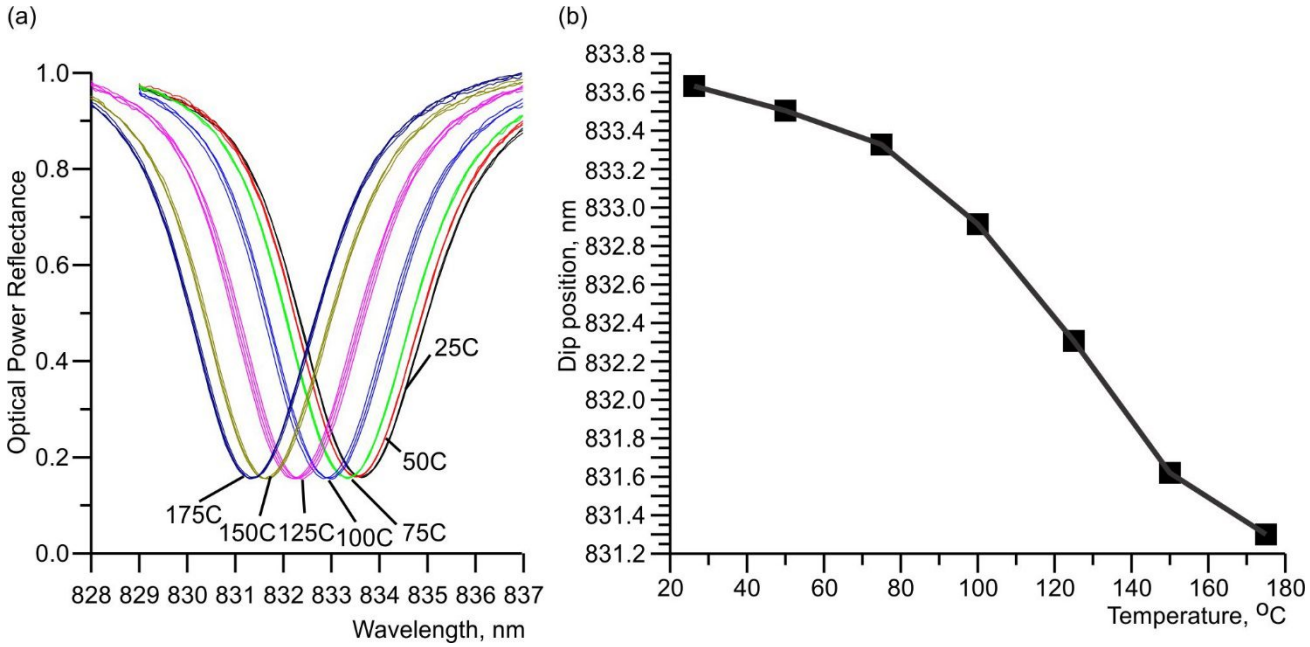

Fig.5 (a) Optical power reflectance spectra of Structure #2 of Fig. 1 containing TiO_2 cavity in the vicinity of the reflectivity dip at various temperatures. (b) Temperature shift of the dip position.

4. DESIGN OF A PASSIVE CAVITY SURFACE EMITTING LASER WITH TEMPERATURE / INSENSITIVE LASING WAVELENGTH

Figure 6(a) depicts the vertical refractive index profile and the vertical profile of the optical field for the designed passive cavity surface emitting laser. The semiconductor part of the device contains a bottom DBR, the active medium placed in one of the DBR layers extended such that the local maximum of the field matches the central plane of the active medium, two layers of GaAlAs with a high Al composition to form oxide confined apertures upon selective oxidation, and a contact layer. Optionally the contact layer can be selectively etched off to eliminate absorption of light in it. The dielectric part of the device contains a transition layer of SiO_2 between the semiconductor structure and the cavity, this layer can also be used for tuning purposes, the $\lambda/2$ TiO_2 cavity and the top DBR formed of 7 pairs of alternating $\lambda/4$ layers of SiO_2 and TiO_2. It should be noted that the optical field profile has a node in the center of $\lambda/2$ TiO_2 cavity, but contrary to all–semiconductor VCSEL, this fact does not create any problems as the active medium is anyway placed in the semiconductor DBR. Due to the shift of the active zone from the cavity to the bottom DBR, the optical confinement factor of the optical field in the active medium is reduced as compared to conventional all–semiconductor VCSEL by a factor of 3. Earlier, an all–semiconductor passive cavity surface emitting laser was fabricated and characterized in Ref. [20], where the shift of the active medium to the DBR led to a similar reduction of the optical confinement factor of the lasing optical mode. It was shown, however, that, despite such reduction, the device revealed stable lasing. Similar, a stable lasing operation can thus be expected from the device designed and presented in Fig. 6(a).

Figures 6(b) and 6(c) show modeled OR spectra of the structure of Fig. 6(a), calculated for two different temperatures, 50°C and 150°C, respectfully. The device was purposely designed such to yield a zero temperature shift of the dip position thus implying the predicted zero temperature shift of the lasing wavelength.

It should be noted here that non–linear behavior of the dip wavelength versus temperature for one of the test structures presented in Fig. 5(b) may lead to the fact that even the optimized device design will still have some non–zero temperature shift of the lasing wavelength. However, this will be significantly smaller than the typical shift in all–semiconductor VCSELs of ~0.07 nm/K.

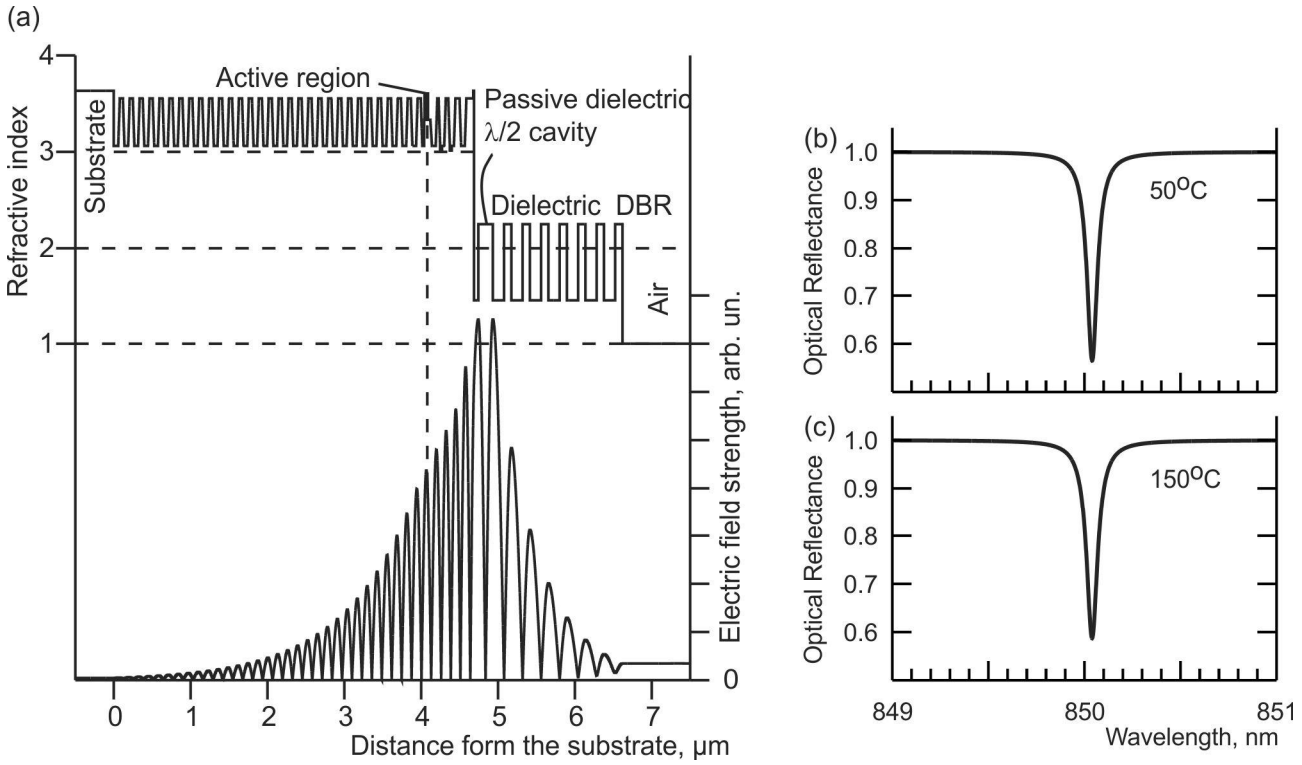

Fig.6 (a) Modeled vertical refractive index profile and optical field profile for a designed passive cavity surface emitting laser. (b) Modeled optical power reflectance (OR) spectrum of the structure of Fig. 6(a) at temperature 50°C. (c) Modeled OR spectrum of the same structure at 150°C.

5. DIELECTRIC STRUCTURES FORMED OF SiO_2 AND Ta_2O_5

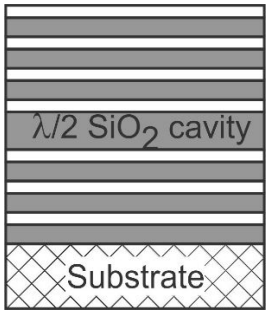

Fig.7. Schematic resonant test structure formed of SiO_2/Ta_2O_5 materials containing λ/2 SiO_2 cavity.

A different pair of dielectric materials, namely SiO_2 and Ta_2O_5 was tested. A resonant structure containing λ/2 resonant cavity formed of SiO_2 placed between a bottom DBR consisting of 3 pairs of alternating λ/4 layers of SiO_2 and Ta_2O_5 and a top DBR containing 3.5 pairs was deposited (Fig. 7). Figure 8(a) shows the OR spectra of the structures measured at two temperatures and revealing a short wavelength shift of the reflectivity dip. Figure 8(b) show these two spectra at a larger magnification in the vicinity of the dip revealing the value of the dip shift: –0.038 nm/K. One should note that the deposition of the structure of Fig. 7 was carried out at a different setup than the deposition of the two structures of Fig. 1. As the refractive indices (and their temperature coefficients) of the dielectric coatings vary upon deposition conditions, it is not possible to use the parameters extracted for SiO_2 from the two structures SiO_2/TiO_2 to analyze the new structure SiO_2/Ta_2O_5. It is however possible to note that in a structure with a thin λ/2 resonant cavity, the contribution of both materials to the temperature shift of the wavelength is comparable. Then, once dn/dT for SiO_2 is positive, like in the structures of Fig. 1, a strong negative contribution of Ta_2O_5 if such would overweight the positive contribution of SiO_2 and result in a shift of the dip towards shorter wavelengths as observed in Figs. 8(a) and 8(b). However, to extract

accurately dn/dT for two materials SiO_2 and Ta_2O_5, investigation of 2 complementary resonant structures SiO_2/Ta_2O_5 with different cavities at the same setup is necessary. Such study will be reported elsewhere.

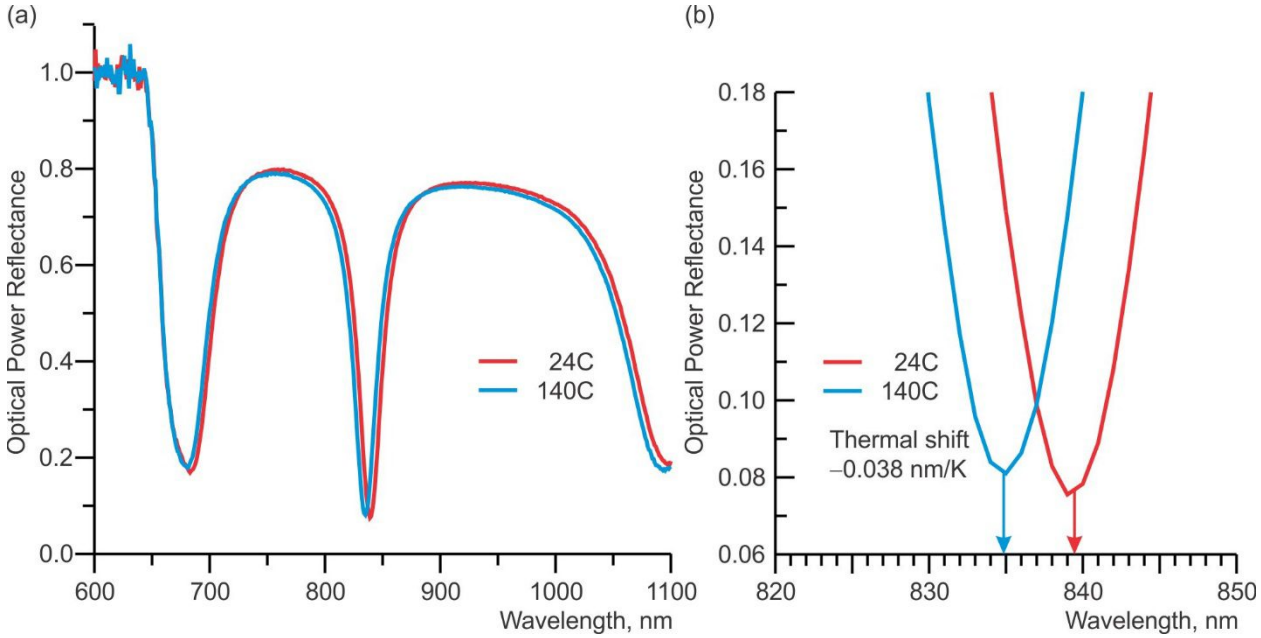

Fig.8. Optical power reflectance spectra of a resonant SiO_2/Ta_2O_5 structure with a $\lambda/2$ SiO_2 resonant cavity. (a) coarse scale. (b) fine scale showing the shift of the reflectivity dip.

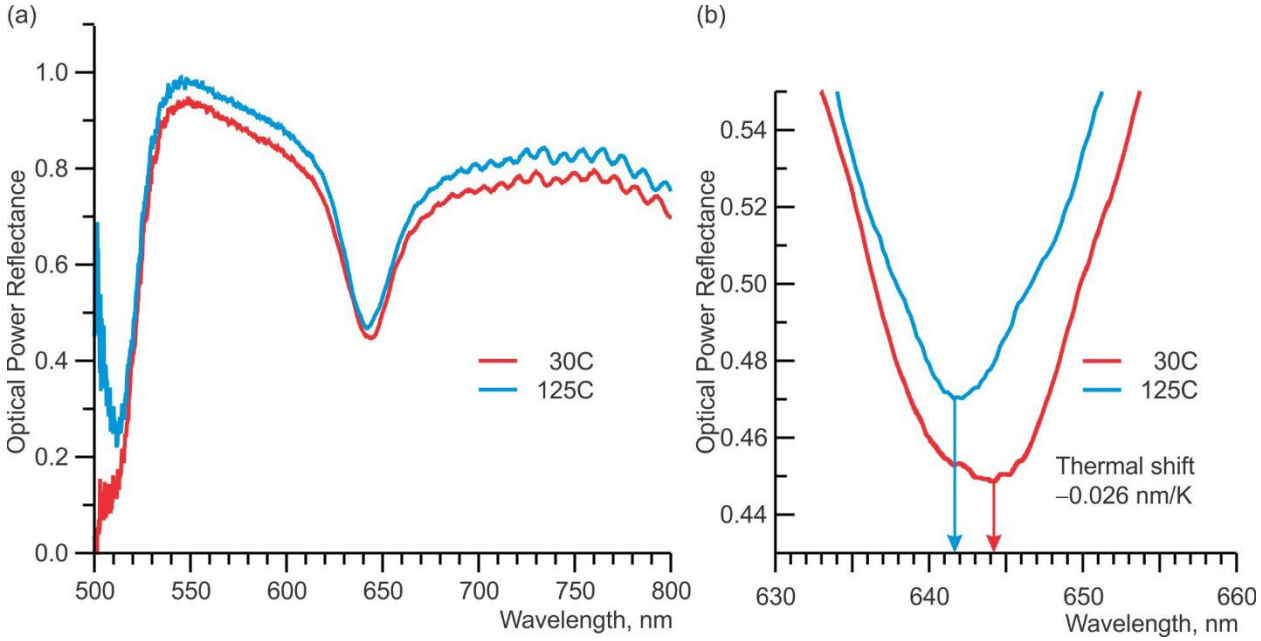

Fig.9. Optical power reflectance spectra of a resonant SiO_2/Ta_2O_5 structure with a $\lambda/2$ SiO_2 resonant cavity designed for 650 nm spectral range. (a) coarse scale. (b) fine scale showing the shift of the reflectivity dip.

Figures 9(a) and 9(b) show the OR spectra of a similar resonant SiO_2/Ta_2O_5 structure with a $\lambda/2$ SiO_2 resonant cavity but designed for the spectral range 650 nm, revealing again a negative shift of the dip at a rate –0.026 nm/K showing that a short wavelength shift of the resonant wavelength upon temperature increase is a rather general phenomenon for dielectric materials used as common coating materials.

6. CONCLUSIONS

To conclude, we have demonstrated that resonant dielectric structures based on common materials used as coatings for semiconductor diode lasers, like SiO_2/TiO_2 or SiO_2/Ta_2O_5 can exhibit short wavelength shift upon temperature increase. Refractive index temperature coefficients for the spectral range 830–930 nm were extracted, $dn/dT = 0.0021\ K^{-1}$ for SiO_2 and $dn/dT = -0.0092\ K^{-1}$ for TiO_2. Negative temperature coefficient of the refractive index enables designing and fabrication of passive cavity surface emitting lasers consisting of a semiconductor bottom DBR, in which the active medium is placed, a dielectric cavity and a top dielectric DBR, and the temperature shift of the lasing wavelength can be on purpose tuned to be positive, zero, or negative. A design of a passive cavity surface emitting laser is proposed for which temperature–insensitive lasing wavelength is predicted. Such devices path the way to wavelength division multiplexing systems with significantly smaller spacing between channels and thus allowing a larger number of channels for a given spectral interval enabling low cost energy efficient uncooled devices.

Acknowledgements: V. A. Shchukin, N. N. Ledentsov, N. Yu. Gordeev, A. M. Nadtochy, A. S. Payusov, M. V. Maximov, S. A. Blokhin, A. A. Blokhin, Yu. M. Zadiranov, N. A. Maleev, and V. M. Ustinov appreciate support from the Russian Science Foundation (Agreement 14–42–00006). T. Slight and W. Meredith appreciate support from the EU FP7 program under Agreement No. 318338 (Project NEWLED).

REFERENCES

[1] J.–R. Kropp, N. Ledentsov, J. Lott, H. Quast, "40 Gb/s Transmission over OM3 Duplex Fiber", IEEE Meeting July 15–17, 2008 Denver, CO, http://www.ieee802.org/3/ba/public/jul08/kropp_01_0708.pdf

[2] J.–R. Kropp, N. Ledentsov, J. Lott, H. Quast, "40 Gb/s and 100 Gb/s Transmission over OM3 Duplex Fiber", IEEE Meeting May 12–15, 2008 Munich, Germany, http://www.ieee802.org/3/ba/public/may08/kropp_01_0508.pdf

[3] http://www.cisco.com/c/en/us/products/collateral/switches/nexus-9000-series-switches/white-paper-c11-729493.html

[4] http://investor.finisar.com/releasedetail.cfm?releaseid=933294

[5] N. N. Ledentsov, V. A. Shchukin, S. S. Mikhrin, I. L. Krestnikov, A. V. Kozhukhov, A. R. Kovsh, L. Ya. Karachinsky, M. V. Maximov, I. I. Novikov and Yu. M. Shernyakov, "Wavelength–stabilized tilted cavity quantum dot laser", *Semicond. Sci. Technol*., Vol. 19, pp. 1183–1188 (2004).

[6] M. B. Lifshits, V. A. Shchukin, N. N. Ledentsov, and D. Bimberg, "Resonance wavelength in planar multilayer waveguides: control and complete suppression of temperature sensitivity", *Semicond. Sci. Technol*., Vol. 22, pp. 380–384 (2007).

[7] S. A. Blokhin, L. Ya. Karachinsky, I. I. Novikov, S. M. Kuznetsov, N. Yu. Gordeev, Yu. M. Shernyakov, A. V. Savelyev, M. V. Maximov, A. Mutig, F. Hopfer, A. R. Kovsh, S. S. Mikhrin, I. L. Krestnikov, D. A. Livshits, V. M. Ustinov, V. A. Shchukin, N. N. Ledentsov and D. Bimberg, "MBE–grown ultra–large aperture single–mode vertical–cavity surface–emitting laser with all–epitaxial filter section", *J. Cryst. Growth*, Vol. 301–302, pp. 945–950 (2007).

[8] N. N. Ledentsov, V. A. Shchukin, and J. A. Lott, in "*Future Trends in Microelectronics: Frontiers and Innovations*", S. Luryi, J. Xu, A. Zaslavsky, eds., Wiley (2013).

[9] A. M. Kasten, S. N. Brown, J. A. Lott, V. A. Shchukin, N. N. Ledentsov, and K. D. Choquette, "Passive Vertical Cavity Surface Emitting Lasers", Proc. IEEE Photonics 2011 (IPC11), Arlington, VA (09–13 October 2011, Paper ThDD5), pp. 919–920.

[10] M. P. Tan, S. T. M. Fryslie, J. A. Lott, N. N. Ledentsov, D. Bimberg, and K. D. Choquette, "Error–Free Transmission Over 1–km OM4 Multimode Fiber at 25 Gb/s Using a Single Mode Photonic Crystal Vertical–Cavity Surface–Emitting Laser," *IEEE Photon. Technol. Lett.*, Vol. 25 (18), pp. 1823–1825 (2013).

[11] R. M. Waxler and G. W. Cleek, "The Effect of Temperature and Pressure on the Refractive Index of Some Oxide Glasses", *J. Research of the National Bureau of Standards – A. Physics and Chemistry*, Vol. 77A (6), pp. 755–763 (1977).

[12] W. J. Tropf and M. E. Thomas, "Infrared Refractive Index and Thermo–optic Coefficient. Measurement at APL", *Johns Hopkins APL Technical Digest*, Vol. 19 (3), pp. 293–298 (1998).

[13] "TIE–19: Temperature Coefficient of the Refractive Index", in: *SCHOTT. Glas Made of Ideas. Advanced Optics*, pp. 1–12, July 2008.

[14] J. Talghader and J. S. Smith, "Thermal dependence of the refractive index of GaAs and AlAs measured using semiconductor multilayer optical cavities", *Appl. Phys. Lett.*, Vol. 66 (3), pp. 335–337 (1995); *ibid*. Vol. 69 (17) p. 2608 (1996).
[15] http://refractiveindex.info
[16] J.–H. Zhao, T. Ryan, P. S. Ho, A. J. McKerrow, and W.–Y. Shih, "Measurement of elastic modulus, Poisson ratio, and coefficient of thermal expansion of on–wafer submicron films", *J. Appl. Phys*., Vol. 85, pp. 6421–6424 (1999).
[17] G. W. McLellan and E. B. Shand, in: *Glass Engineering Handbook*, 3rd edition (McGraw Hill, New York 1984), pp. 2-14–2-15.
[18] http://www.azom.com/properties.aspx?ArticleID=1179
[19] http://www.almazoptics.com/TiO2.htm
[20] J. A. Lott, V. A. Shchukin, N. N. Ledentsov, A. M. Kasten, and K. D. Choquette, "Passive cavity surface emitting laser", *Electron. Lett*., Vol. 47 (12), pp. 717–718 (2011).